Journal of Molecular Liquids 323 (2021) 115094

Contents lists available at ScienceDirect

Journal of Molecular Liquids

journal homepage: www.elsevier.com/locate/molliq

Fabrication and characterisation of electrospun Polycaprolactone/Polysuccinimide composite meshes

Constantinos Voniatis [a,b], Dóra Barczikai [a], Gergő Gyulai [c], Angela Jedlovszky-Hajdu [a,*]

[a] Laboratory of Nanochemistry, Department of Biophysics and Radiation Biology, Semmelweis University, Budapest, Hungary
[b] Department of Surgical Research and Techniques, Semmelweis University, Budapest, Hungary
[c] Laboratory of Interfaces and Nanostructures, Eötvös Loránd University, Budapest, Hungary

ARTICLE INFO

Article history:
Received 28 September 2020
Received in revised form 8 December 2020
Accepted 14 December 2020
Available online 28 December 2020

Keywords:
Co-electrospinning
Blend electrospinning
Layered electrospinning
Fibrous composite meshes
Polycaprolactone
Polysuccinimide

ABSTRACT

The following manuscript presents the first attempt to fabricate and characterise electrospun polycaprolactone/poly(succinimide) composite meshes. While each material has its own advantages, a composite mesh could provide further options in the wide and diverse application spectrum of electrospun fibrous membranes. Polycaprolactone is a well-known polymer with excellent mechanical properties and a resistance against most chemicals. On the other hand, poly(succinimide) is an easily modifiable polymer that could provide functionalisation options to the system, giving rise to new and perhaps better alternative solutions, for example in the sensors field. Additionally, as both polymers are biocompatible and biodegradable the system could be an especially advantageous option in the environmental and biomedical fields as well. Three different meshes were produced by utilizing three different electrospinning configurations: a. Electrospun layered meshes, b. Co-electrospun meshes and c. Blend electrospun meshes. Physical-chemical (Attenuated Total Reflectance Fourier Transform Spectrometry, Scanning Electron Microscopy, Fluorescence Microscopy, Water Contact Angle), as well as mechanical characterisation, were performed validating the proof of concept for the three composite meshes. Furthermore, PCL/PSI meshes proved mechanically stronger as they exhibited almost double the loading capacities when compared to PSI only meshes. Wettability studies on the other hand proved that addition of a PSI component will decrease the water contact angle and therefore make the wettability nature of the composite meshes more favourable for biomedical applications.

1. Introduction

Material science is undoubtedly an interdisciplinary science. Whether biomedical, environmental or other, material science has always been a central point in scientific research. One of its most intriguing focus are composite materials. Combining two materials is always an exciting yet highly challenging task [1]. Naturally, each material whether metal, polymer or ceramic has its own advantages and disadvantages. By combining different materials scientists have tried to overcome issues or limitations presented by the use of single based materials and seek possible synergistic effects the component materials might elicit with each other. Until the past decades, the primary objective of a composite material was to physically and mechanically reinforce the weaker component material that had other advantageous features (e.g. chemical, thermal etc.) [2–4]. Currently researchers, regardless of scientific field, aim to synthesize and produce complex, intricate and functionalized materials incorporating not only different component materials but different physical systems as well (e.g. nanoparticles, nanotubes, etc.) providing new options for a plethora of applications [4,5].

Electrospinning is a widely known method to produce membranes or meshes composed of micro- or nanosized fibres. Quite frequently described as a "simple and versatile technique", electrospinning does indeed provide numerous options to complement or enhance the membrane production. Production of composite membranes is possible by utilizing different electrospinning configurations (e.g. layer electrospinning, co-electrospinning, blend electrospinning, multi-nozzle systems, coaxial spinnerets etc.) which consequently results in meshes composed of two or more polymers [6–8]. However, the system's microstructure and therefore physical or mechanical properties vary according to the applied method. Layer electrospinning is a sequential process where different polymers are electrospun one after the other, producing a mesh that is composed of two or more layers. Naturally, each layer is composed of only one type of polymer fibre. In contrast, a *co*-electrospun mesh is fabricated by electrospinning two different polymers simultaneously. The fabricated mesh is composed of two different polymer fibres randomly interpenetrating the entire mesh. Blend electrospinning requires mixing the two polymers before the electrospinning itself. If the solvents of the two polymers are miscible

* Corresponding author at: Nagyvárad square 4, 1089 Budapest, Hungary.
E-mail address: hajdu.angela@med.semmelweis-univ.hu (A. Jedlovszky-Hajdu).

https://doi.org/10.1016/j.molliq.2020.115094

and no phase separation occurs, the blend solution (containing the two polymers) can be electrospun resulting in a mesh composed of fibres containing both polymers. If the polymer solutions are immiscible, and their viscosity is similar, fibres composed of an inner core and outer sheath layer comprised of the two polymers can be achieved in some cases (after extensive optimization) without the requirement for specialized spinnerets (coaxial needle) [9–11].

Polycaprolactone is probably one of the most popular polymers researchers have been investigating in recent years [1,12–14]. It is a biodegradable, semi-crystalline, aliphatic polyester, synthesized by ring-opening polymerization of ε-caprolactone. PCL demonstrates resistance to most organic solvents and has excellent mechanical properties. It has numerous applications in the biomedical (e.g. suture material, drug delivery system) [15], environmental (e.g. additive to plasticizers, hydrophobic agent) [16] and even in the sensor (e.g. strain sensor, vapour sensors) [17] and filter (e.g. aerobic filter) [12] fields.

Poly(succinimide) on the other hand, is a polyimide that recently gained increased attention due to its versatile nature as it can be easily modified and functionalized due to the monomer's imide group. Synthesized by the thermal polycondensation of L-aspartic acid, PSI is implemented in filters, chelator agents, fertilizers and other environmental applications [18,19]. Furthermore, being biocompatible and rapidly biodegradable it has recently earned the interest of the biomedical field demonstrating promising potential as a drug delivery system and tissue engineering scaffold [20,21].

Electrospun PCL meshes have been investigated extensively while only a limited number of electrospun PSI studies can be found in the literature [22–24]. To our knowledge, a PCL/PSI composite mesh has never been investigated. Combining the two polymers could provide new options or even solutions in a broad spectrum of applications. For example, PCL could provide mechanical and structural support for PSI chelators, filters, and sensors Additionally, in the biomedical field, PSI could provide several options to modify and functionalize PCL implants. Both polymers are biocompatible and biodegradable. PCL biodegradation is well documented. It occurs in two phases: a) hydrolysis of the aliphatic ester and b) caproic acid is either metabolised in the tricarboxylic acid cycle or eliminated via renal secretion [25]. On the other hand PSI in a mildly alkaline environment (e.g. physiological pH) is hydrolysed to polyaspartic acid and then is enzymatically degraded [26].

The following manuscript presents the fabrication of PCL/PSI meshes by three different electrospinning configurations (layered electrospinning, co-electrospinning, blend electrospinning) and their physical-chemical (Attenuated Total Reflectance Fourier Transform Spectrometry, Scanning Electron Microscopy, Fluorescence Microscopy, Water Contact Angle) and mechanical (uniaxial tension testing) characterisation.

2. Experimental section

2.1. List of materials

Polycaprolactone (Mw ~80,000, Sigma Aldrich, USA), L-Aspartic Acid (Reagent Grade ≥ 98%, Mw ~133, Sigma Aldrich, USA), Orthophosphoric Acid (Reagent Grade ≥ 99%, Mw ~98, Sigma Aldrich, USA), Dimethylformamide (Anhydrous, Reagent Grade 99.9%, VWR International), THF (anhydrous, ≥99.9%, inhibition free, Sigma Aldrich, USA), Nile Blue A Stain (Dye Content ≥75%, Sigma Aldrich, USA).

2.2. PSI synthesis

L-aspartic acid and phosphoric acid were mixed at a 1:1 ratio and mixed in a rotary vacuum evaporator system (RV10 digital rotary evaporator, IKA, Germany). The mixture was gradually heated up to 180 °C using a silicon oil bath while the pressure inside the flask was gradually decreased to 5 mbar. The synthesis duration was eight hours. Further details about the synthesis and quality control of the synthesized PSI can be found in the research group's previous works [22,27].

2.3. Polymer solution preparation

PCL solutions were prepared by mixing 1 g of PCL pellets in a 1:1 DMF-THF solution with a final 15 *w*/w % concentration. While PSI solutions were prepared by mixing 1 g of the synthesized PSI in DMF with a final 25 *w*/w % concentration. For the blend electrospinning, the two polymer solutions (15 w/w % PCL/DMF-THF and 25 w/w % PSI/DMF) were first prepared separately, then were subsequently mixed thoroughly until a homogenous blend solution was achieved. The mass ratio of PCL/PSI in the blend solution was 1:1.

2.4. Electrospinning

Polymer solutions were transferred to 5 mL Luer slip-syringes (Chirana, Slovakia) equipped with customized 21G needles (Becton Dickinson, USA). Polymer solutions then were delivered by an infusion pump (KDS100, KD Scientific, USA) at a constant flow rate. The electric potential was provided by a high voltage DC supply (73030P series, Genvolt, UK). Every mesh was fabricated by using two oppositely placed, separate needle systems, from a 20 cm collector distance, at a 25 ± 2 °C temperature and 30 ± 10% humidity. Two rotating collector speed were examined 500 and 3000 RPM. All composite membranes were fabricated having a final equal amount of PCL and PSI (1:1 mass ratio). Layered electrospinning was performed by electrospinning a PSI layer directly after having electrospun the PCL layer (Fig. 1). In the case of the co-electrospun meshes, fabrication was performed by concurrently electrospinning PCL and PSI from two oppositely placed needles. As the electrospun volume was different for the two polymer solutions (one being 15 *w*/w %, the other 25 w/w %), the PSI solution flow rate was adjusted (Table 1) to achieve a balanced distribution of the 1:1 PCL/PSI mass ratio. For the blend electrospinning, after mixing the two polymer solutions, the blend solution was divided and transferred to the syringes (Fig. 1). Control meshes (PCL-only and PSI-only meshes) were also prepared as a reference. The exact electrospinning parameters can be found in Table 1.

2.5. ATR-FTIR analysis

Chemical analysis of the electrospun fibrous meshes was performed using an FTIR spectrophotometer (4700 series type A, JASCO, Japan), equipped with a diamond ATR head (ATR Pro One, JASCO, Japan). All measurements were carried out in a mid-infrared range of wavelength (4000–400 cm^{-1}), with 2 cm^{-1} resolution and 126 total number of scans. Before sample analysis, background spectra (H_2O, CO_2, ATR Head exclusion) were obtained on a clean and dry diamond crystal and was subtracted from the sample spectra.

2.6. Scanning electron microscopy

Small samples (25 mm2) were cut from all the meshes. Images were taken with a JSM 6380LA scanning electron microscope (JEOL, Japan). After securing them on an adaptor with conductive stickers, samples were subsequently coated with a thin layer of gold using a JFC-1200 Sputter Coating System (JEOL, Japan). The applied voltage was 15 kV and micrographs were obtained at a 1000×, 2500× and 5000× magnifications. Average fibre diameter and size distribution were determined by measuring 100 individual fibres. All measurements and studies were performed using Fiji software (Open Source Software) and a non-parametric one-way ANOVA analysis (Kruskal-Wallis test) was performed using STATISTICA 10 software (TIBCO Software Inc., USA) ($p < 0.05$).

2.7. Fluorescence microscopy

Imaging was performed on the co-electrospun and blend electrospun meshes using a Nikon Eclipse E600 Fluorescence Microscope

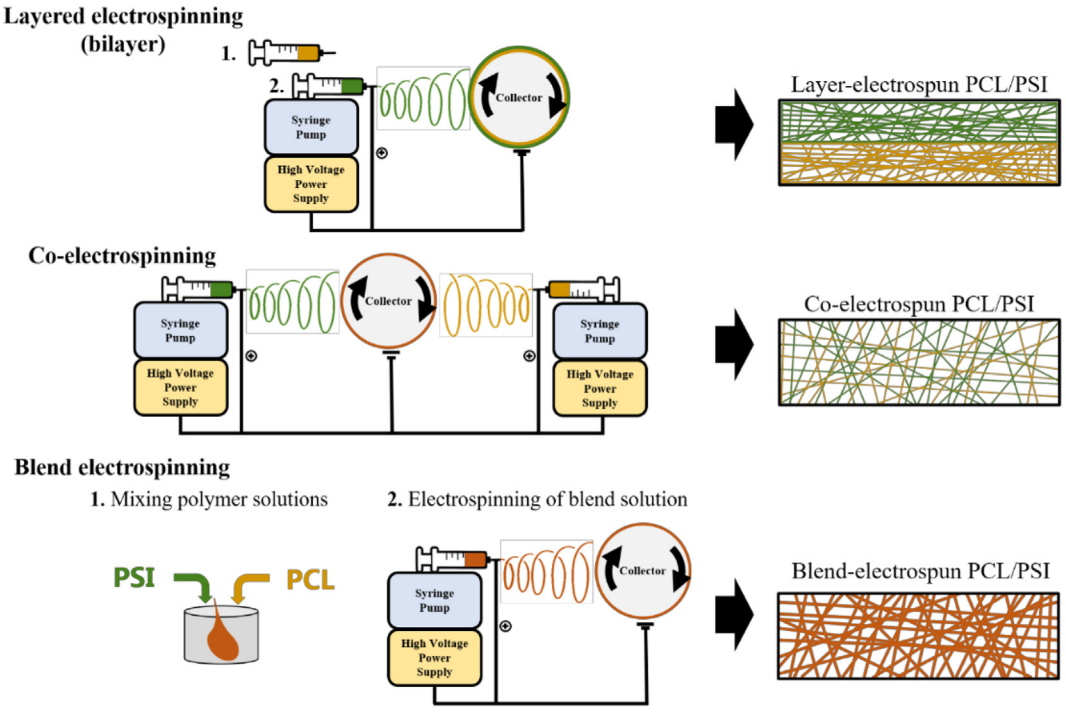

Fig. 1. Schematic of the preparation and electrospinning configuration for the fabrication of the different composite meshes.

Table 1
Composite and single polymer mesh electrospinning parameters (20 cm collector distance, 500 and 3000RPM collector speed).

Mesh	Solution concentration (w/w%)	Voltage (kV)	Flow rate (ml/h)
PCL	15	12.5	1
PSI	25	13.5	1
Layered electrospun PCL/PSI	15 / 25	12.5 /13.5	1/1
Co-electrospun PCL/PSI	15 / 25	12.5 / 13.5	1/0.6
Blend electrospun PCL/PSI	15 + 25	13	1

(Nikon, Japan) equipped with a Prime BSI Scientific CMOS (Teledyne Photometrics, USA). A small sample was collected during electrospinning which then was observed under the microscope at 380 and 480 nm wavelengths. In order to distinguish the PCL from the PSI fibres, Nile Blue stain was thoroughly mixed over 72 h (0.5 *w*/w %) with the PCL solution. For the blend electrospinning, the dyed PCL solution was mixed with the PSI solution for 5 min before electrospinning.

2.8. Wettability assessment

Assessment of wettability was performed on small circular samples from each kind of setup (d = 1.5 cm). Distilled water was transferred to a 50 μl Hamilton syringe with a 0.56 mm needle then, a droplet (5 μl) was carefully placed on the centre of the samples. Assessments were performed using a contact angle meter with a built-in camera (OCA 15 Plus, Dataphysics, Germany). Initial water angles (θ) were measured as well as absorption times (t) when applicable. In the case of the layered samples, the contact angle was measured on both sides.

2.9. Mechanical characterisation

Mechanical performance (e.g. tensile strength, elasticity, elongation etc.) is one of the most crucial parameters of any material. To perform mechanical studies, rectangle samples (2 cm × 6 cm) were prepared from every mesh. Samples of both horizontal ($N = 5$) and vertical ($N = 5$) direction to the direction of the rotating collector were measured. For the study, a uniaxial mechanical tester (4952, Instron, USA) was used. After clamping the samples along their shorter sides, samples were pulled until tearing. Pulling speed was set at 1 mm/min. The highest load registered was regarded as the maximal sustained load. A specific loading capacity was then calculated using the following formula:

$$\textit{Specific Load Capacity}\left(\frac{N\,m^2}{g}\right) = \frac{\textit{Maximal Sustained Load}\ (N)}{\textit{Area Density}\left(\frac{g}{m^2}\right)}$$

where

$$\textit{Area Density}\left(\frac{g}{m^2}\right) = \frac{\textit{Sample Mass}\ (g)}{\textit{Sample Surface}\ (m^2)}$$

A non-parametric one-way ANOVA analysis (Kruskal-Wallis test) was performed on the Specific Load Capacities using STATISTICA 10 software (TIBCO Software Inc., USA) ($p < 0.05$).

3. Results and discussion

3.1. Electrospinning

Electrospinning of the composite meshes was performed without any of them presenting any issues while none of the setups exhibited individual peculiarities. No gelation at the tip of the needle, spitting, dripping or interference between the two polymers was observed in any of the configurations. Removal of the meshes from the collector presented no difficulties and no changes were observed throughout their storage and characterisation. All fabricated meshes were produced with a final 1:1 mass ratio of PCL to PSI. A minimal amount of material loss was observed as in any form of electrospinning. The lost material was regarded as negligible. Macroscopically all meshes look identical. However, upon a closer inspection, a small difference can be observed. PCL fibres are rigid and adhere well together while PSI fibres are light and fleecy (Fig. S1).

3.2. ATR-FTIR analysis

The chemical characterisation of the meshes was conducted by ATR-FTIR. Results do indeed confirm the presence of the two polymers in all composite meshes (in the case of the bilayer mesh, chemical characterisation was performed on both sides of the sample) (Fig. 2). Specifically, the typical PCL peaks at approximately 2950 cm^{-1} and 2860 cm^{-1} marking the asymmetric and symmetric CH_2 stretching, the peak at 1730 cm^{-1} marking the carbonyl stretching, the peak at 1190 cm^{-1} marking the OC–O stretching and the peak at approximately 800 cm^{-1} for the C–H bending are visible [28–30]. Additionally, the main PSI peaks: a. 3596 cm ^{1} for the O–H groups, b. 2961 cm^{-1} for the C–H bonds c. 1709 cm^{-1} (asymmetric stretching vibration) and 1393 cm^{-1} (stretching bending vibration) for the imide ring. and at approximately 1200 cm-1 for the C–N (stretching vibration) are visible as well [22,31,32]. FTIR results of the single polymer meshes can be found in the supplementary information (Fig. S2).

3.3. Scanning electron microscopy

The fibrous microstructure of the meshes was confirmed by utilizing scanning electron microscopy. As seen in Fig. 3, all composite meshes are indeed fibrous (Micrographs and fibre analysis results of the single polymer meshes can be found in the supplementary information Fig. S3-S4). No fibre deformation (beads) or fusion can be seen in any of the meshes. Interestingly, PCL and PSI fibre morphology seems to be different in both the single component meshes (PCL, PSI) and in the separate layers of the layered PCL/PSI mesh. While PCL fibres tend to be flexuous, adhering together in groups, PSI fibres are straight with less inter-fibre adherence. Therefore, regarding fibre-fibre interactions, the two fibre types exhibit different properties.

The average fibre diameters of the PCL and PSI fibres in the layered mesh at 500RPM (slow rotating collector) (Fig. 4) are similar to the fibre diameters (d = 450–650 nm) obtained in previous works of our research group and others as well [22,24,33]. Important to note, that in the case of the co-electrospun mesh, even though some fibres could be recognized as PCL or PSI fibres, we cannot accurately classify fibres according only to visual data (i.e. size, morphology). Therefore, average fibre diameter calculations were performed regarding the two fibres composing the mesh as one system. Nevertheless, the average calculated diameter is between the PCL (d = 560 ± 190 nm) and PSI (d = 510 ± 120 nm) fibre size range (single polymer diameter analysis results can be found in the supplementary information). An additional interesting point is that fibre diameter increases in the blend-electrospun meshes compared to the other composite meshes.

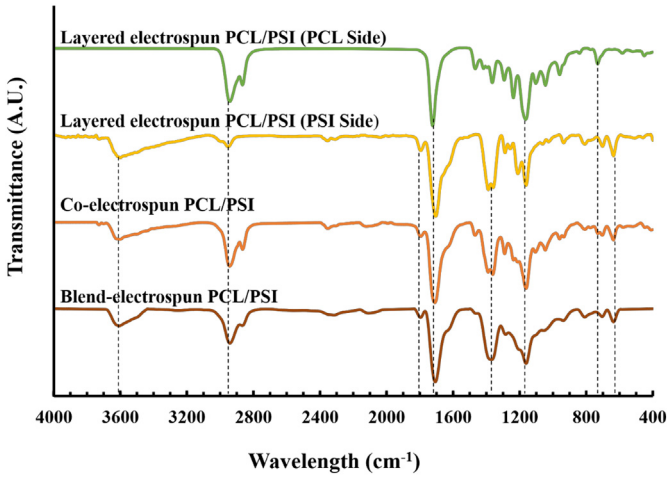

Fig. 2. FTIR analysis of the PCL/PSI composite meshes.

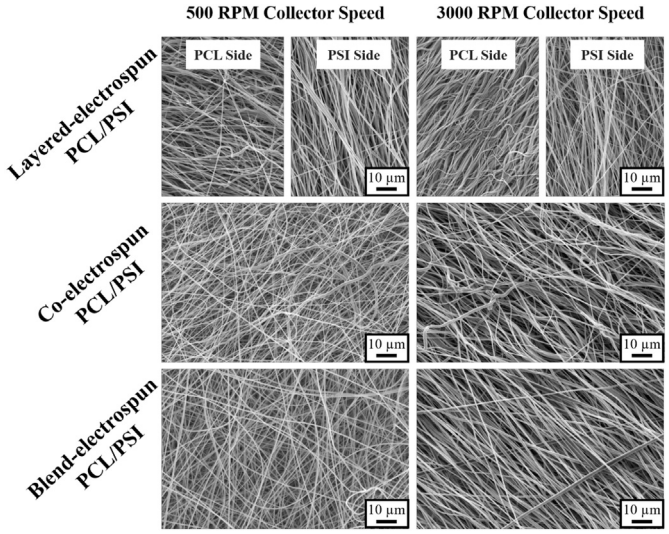

Fig. 3. Results of the scanning electron microscopy.

Overall research of the collector speed increase from 500 to 3000 RPM had two effects: 1. a decrease in fibre diameter is observable (based on the statistical analysis) (Fig. 4) and 2. a slight increase in fibre alignment based on SEM micrographs (Fig. 3).

In every composite mesh, the fibre size falls in the middle of the nanometre – micrometre spectrum. Fibres of this size closely resembling collagen fibres (tropocollagen ≈ 300 nm – collagen fibrils ≈1 μm) [34] and can be utilized in wound dressing applications, as well as tissue engineering applications for soft and hard connective tissues [14,34–36]. Depending on the exact application, i.e. soft tissue, tendon, or bone regeneration the fibre diameter can be adjusted in the future by altering either the solution or electrospinning parameters.

3.4. Wettability assessment

Wettability studies were performed to examine the composite meshes as the component materials behave almost exactly opposing,

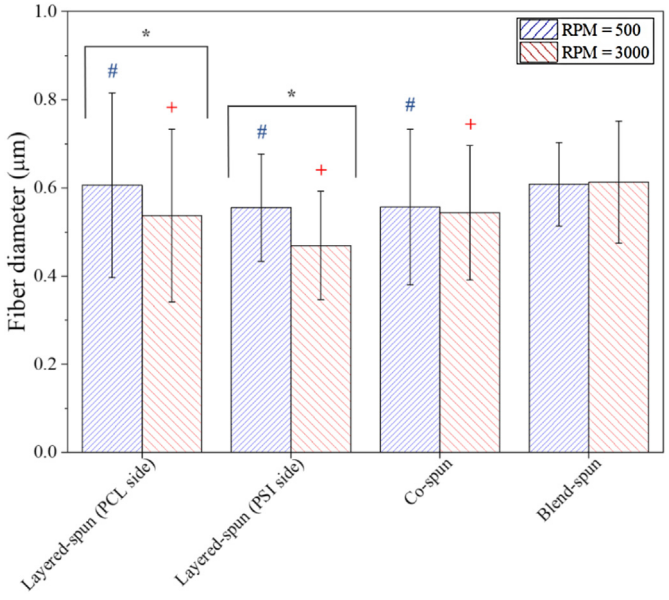

Fig. 4. Fibre diameter analysis results: *p < 0.05 between 500 and 3000 RPM meshes (between similar types of mesh); # p < 0.05 compared to the blend electrospun (500 RPM) mesh, +p < 0.05 compared to the blend electrospun (3000 RPM) mesh.

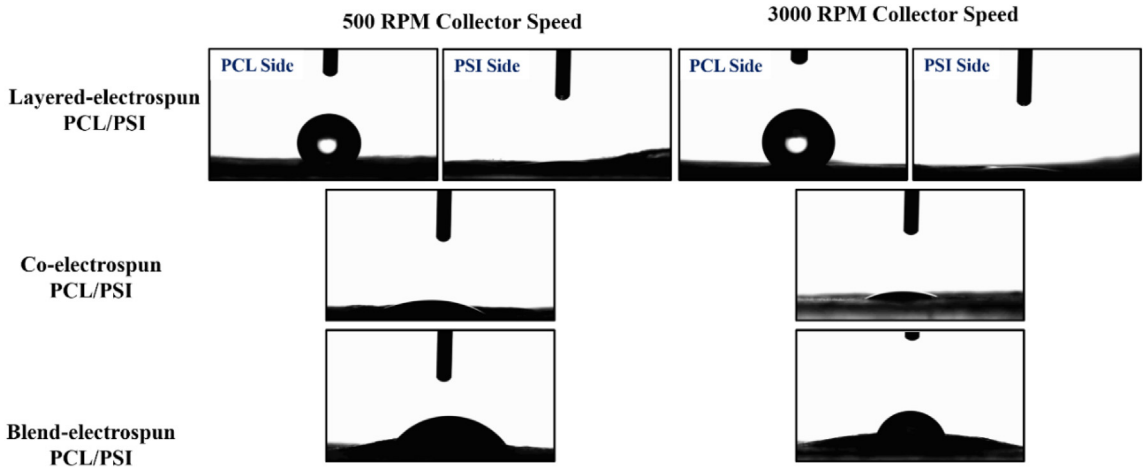

Fig. 5. Initial water contact angles of the composite PCL/PSI meshes.

PCL fibres being typically hydrophobic [37] whereas PSI fibres being hydrophilic [24]. Control measurements confirmed this hypothesis as PCL exhibit a hydrophobic nature ($\theta \geq 90°$) contrary to PSI where the water droplet is almost pulled inside the mesh and only an initial water contact angle could be measured (Fig. 5, Supplementary Videos). Interestingly, the layered electrospun PCL/PSI mesh exhibited this dual nature as the PCL side is hydrophobic while the PSI side is hydrophilic (Fig. 5 and Table 2). The initial water angle measured on the co-electrospun meshes ($\theta = 129.2°$, $t = 3.22$ s;) is quite different from the one measured for blend electrospinning ($\theta = 109.5°$, $t = 7.55$ s) and so was the absorption time (less than half) (Table 2, Supplementary Videos). These results suggest that although the basic chemical composition of these meshes is the same, the microstructure and distribution of the polymers within the mesh is different further indicating that the *co*-electrospun meshes are composed of two different polymer fibres within one mesh while the blend electrospun meshes are composed of two polymers within one fibre. In addition, examining Table 2 when comparing the 500 RPM to their 3000 RPM counterparts water angle (θ) is increased while the absorption time (t) is decreased in every case. These results indicate that an increase in the collector speed, increases the orientation of the fibres and therefore decreases the overall porosity of the meshes. Unequivocally, the wettability studies proved crucial as they demonstrate the differences in porosity amongst the composite meshes which can give some insight regarding in vivo tissue integration [38].

In the future, these features can be adjusted according to a specific application. For example, in biomedical applications, this composite

Table 2
Water contact angles and water absorption times of the single polymer and composite meshes.

Mesh	θ (°)	t (s)
Layered PCL/PSI (500 RPM) – PCL Side	131.8 ± 6.1	–
Layered PCL/PSI (500 RPM) – PSI Side	31.7 ± 2.0	1.41 ± 2.37
Layered PCL/PSI (3000 RPM) – PCL Side	128.9 ± 2.6	–
Layered PCL/PSI (3000 RPM) – PSI Side	48.7 ± 6.1	3.75 ± 0.90
Co-electrospun PCL/PSI (500 RPM)	129.2 ± 5.8	3.22 ± 10.37
Co-electrospun PCL/PSI (3000 RPM)	138 ± 5.1	3.2 ± 10.37
Blend PCL/PSI (500 RPM)	109.5 ± 3.2	7.55 ± 5.5
Blend PCL/PSI (3000 RPM)	116.75 ± 8.4	18.8 ± 11.8

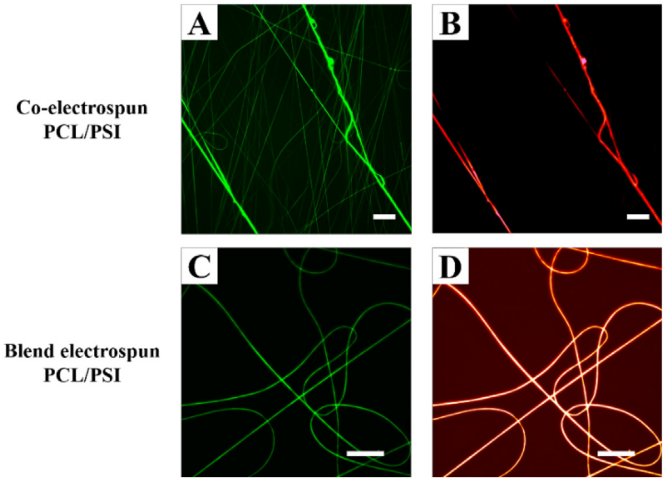

Fig. 6. Fluorescent microscopy imaging: Co-electrospun PCL/PSI at 380 nm (A), 480 nm (b) wavelength Blend electrospun PCL/PSI at 380 nm (C) and 480 nm (D). (Scale bar: A/B – 20 μm, C/D – 50 μm).

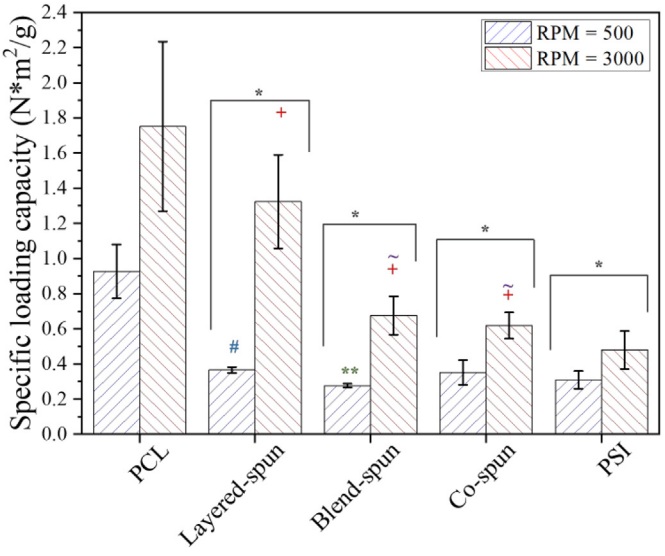

Fig. 7. Mechanical evaluation results of vertical mesh samples; *$p < 0.05$ between 500 and 3000 RPM meshes (between similar types of mesh); # $p < 0.05$ compared to PSI-only500 RPM mesh; + $p < 0.05$ compared to the PSI-only 3000 RPM mesh; ** $p < 0.05$ compared to the layered-spun 500 RPM mesh; ~ $p < 0.05$ compared to the layered-spun 3000 RPM mesh and! $p < 0.05$ compared to the Co-spun 500 RPM mesh.

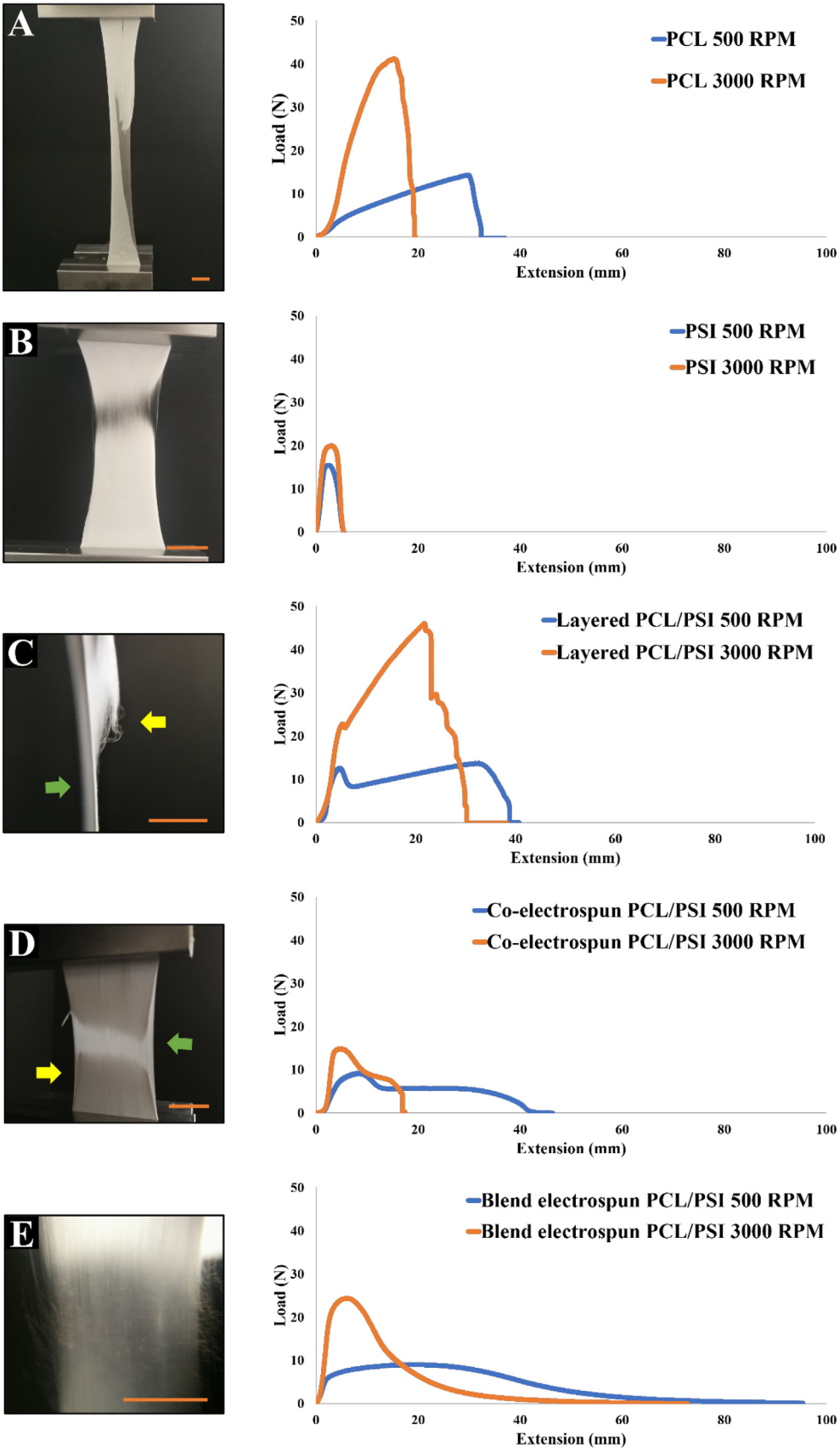

Fig. 8. Macroscopical differences and characteristic vertical sample stress-strain curves of the PCL (A), PSI(B), Layered electrospun PCL/PSI (C), Co-electrospun PCL/PSI (D) and Blend electrospun PCL/PSI (E) Meshes (Scale bar at 1 cm, green arrows indicating PCL fibres, yellow arrows indicating PSI fibres).

matrix could be a promising tissue scaffold. Two of the most frequent challenges in this area are mechanical strength and cell infiltration. PCL has been regularly utilized as a tissue scaffold being biodegradable and mechanically robust yet its major disadvantage is the poor cellular infiltration due to its high hydrophobicity. Some tactics have been already utilized in the endeavour of circumventing this issue [39,40] yet they seem to always have disadvantages (additional or complicated processing steps, alteration of the original system, higher production costs). On the contrary, the PCL/PSI meshes not only circumvent this issue without requiring additional processing but can also be further modified (increasing collector speed, PCL/PSI ratio, PSI cross-linking) to further adjust these parameters but have the potential to be additionally functionalized as both polymers have been modified in the past (e.g. nanoparticle addition, drug encapsulation) providing further advantages to the system.

3.5. Fluorescence microscopy

Fluorescent microscopy was utilized to additionally visualize the difference between the co-electrospun and blend electrospun meshes. At the examined wavelengths (380 and 480 nm) while PSI demonstrated fluorescent properties, PCL did not (Fig. S5). Nile Blue dye was utilized to stain the PCL fibres, a method previously utilized by the research group [24]. After staining, both polymers were visible, emitting a fluorescent green light at 380 nm wavelength, (Fig. S5). The two fibres are visible also through the 480 nm filter, however, the PCL stained fibres also emit in red. In Fig. 6A, the green fluorescent light derives from the two polymers whereas in Fig. 6B the red fluorescent light (due to the Nile Blue staining), shows only the PCL fibres. While in Fig. 6A–B (*co*-electrospinning setup) the two polymer fibres are individually visible, in Fig. 6C–D (blend setup) are not (even though the dye was thoroughly mixed with the PCL solution). These results further suggest that the blend electrospun meshes are truly composed of two polymers within one fibre.

3.6. Mechanical characterisation

Mechanical studies were indispensable. Firstly, the increase in the specific loading capacity in the vertical samples due to fibre alignment is evident as in every case the meshes produced on the 3000 RPM collector were found to be significantly stronger than their 500 RPM counterparts (Fig. 7). As expected, the addition of PCL significantly enhanced the mechanical properties of the composite meshes when compared to the control PSI meshes (Fig. 7). The layered electrospun mesh proved to be the strongest composite mesh while the blend meshes the weakest. Perhaps an interesting point is that while blend meshes proved weaker than co-electrospun meshes, they had a narrower standard deviation. Therefore, even if they are weaker, blend meshes seem to have more reproducible mechanical properties compared to *co*-electrospun meshes where the distribution of the two different polymer fibres makes the mesh prone to larger performance deviations.

Accordingly, when increasing the collector speed the horizontal samples become weaker as fewer fibres are oriented towards the horizontal direction (Fig. S6). Furthermore, fibre alignment also decreases the overall extension (Fig. 8) as aligned fibres (being already stretched to some extent) can extend less than coiled or undulating fibres. Additionally, in Fig. 8 the different behaviour exhibited by the single polymer and composite meshes can be observed. Observing the layered electrospun meshes an initial peak can be found marking the tear of the PSI layer following by an increase until the PCL layer is also torn (Fig. 8C). This is visible due to PCL being more elastic (Fig. 8A), resulting in the PSI fibres being torn while the PCL fibres are still elongating. In the case of the co-electrospun meshes, the initial peak is higher the secondary peak (Fig. 8D). The tear of the PSI fibres is not visible as they are overshadowed by the PCL fibres, after which the additionally. Extension of the PCL fibres is visible. As there are no chemical bonds between the fibres, the reason of the difference in the stress-strain curve shape is probably due to the physical forces holding the fibres together (friction between the fibres) being different. The hypothesis is that PCL-PCL inter-fibre connection is probably stronger than a PCL-PSI inter-fibre connection). Furthermore, the blend electrospun mesh stress-strain curve (Fig. 8E) resembles the curves produced by single component meshes (one peak) thus further suggesting that the mesh is composed of homogenous fibres containing both polymers. Some macroscopically visible differences can be macroscopically observed when the meshes are under high tension revealing the methodology used for their fabrication (Fig. 8A–E).

Comparing the meshes to other composite systems their mechanical parameters show a similar tendency typically when one of the two components is weaker. In that case, a decrease in mechanical performance is observed, for example when combing PCL with gelatine or collagen [1,24,41,42]. The current mechanical strength of the composite PCL/PSI meshes is adequate for in vivo implantation, something we would like to demonstrate in a future work. Nevertheless, if required, the mechanical properties of the meshes can be adjusted or enhanced by altering the PCL/PSI ratio or other methods (e.g. cross-linking, heat treatment) [23,43].

4. Conclusion

In this manuscript, we present three feasible and reproducible methods to fabricate electrospun composite Polycaprolactone/Poly (succinimide) meshes. The chemical, physical and mechanical characterisation conclusively demonstrated that the three meshes even if composed of the same two polymers, while having technically the same chemical composition, exhibit different physical and mechanical attributes due to their differences in fabrication methods and consequently microstructure. The three composite meshes are composed of nanofibres in the 500–600 nm range. Overall, the addition of PCL proved effective in increasing the mechanical performance of a PSI based system (Layered-electrospun PCL/PSI proved 2.5 stronger) while the addition of PSI succeeded in decreasing the hydrophobicity of a PCL based system. All composite meshes were fabricated having a 1:1 PCL /PSI mass ratio thus altering this ratio and further optimisation could prove beneficial as mesh parameters, as well the advantages of each composite mesh could be further enhanced to serve different objectives intended for different applications. Polymer ratios, fibre diameters even the microstructure can be adjusted. These modifications give rise to numerous possible new systems, from the addition of drugs and nanoparticles to 3D electrospun structures each of them being equally promising and exciting.

Supplementary data to this article can be found online at https://doi.org/10.1016/j.molliq.2020.115094.

Author statement

Constantinos Voniatis (Methodology, Formal analysis, Validation, Visualization, Writing-original draft, Writing- review&editing); Dora Barczikai (Visualization, Writing-original draft); Gergo Gyulai (Visualization, Investigation); Angela Jedlovszky-Hajdu (Conceptualization, Supervision, Funding acquisition, Resources, Writing-original draft, Writing-review&editing).

Declaration of Competing Interest

The authors confirm that this work is entirely original and no part of it has been published elsewhere, nor it is currently under consideration for publication elsewhere. We declare that there are no known conflicts of interest associated with this publication and there has been no financial support for this work that could have influenced its outcome.

Acknowledgements

This work was supported by the National Research, Development and Innovation Office (NKFIH FK 124147), the János Bolyai Research

Scholarship of the Hungarian Academy of Sciences (JHA) and by the new national excellence program of the Ministry for Innovation and Technology (ÚNKP-19-4-SE-04, ÚNKP-20-5-SE-9). The research was further financed by the Higher Education Institutional Excellence Programme of the Ministry for Innovation and Technology in Hungary, within the framework of the Therapeutic Development thematic programme of the Semmelweis University. This work was completed in the ELTE Institutional Excellence Program (1783-3/2018/FEKUTSTRAT) supported by the Hungarian Ministry of Human Capacities.

References

[1] M.J. Mochane, T.S. Motsoeneng, E.R. Sadiku, T.C. Mokhena, J.S. Sefadi, Morphology and properties of electrospun PCL and its composites for medical applications: a mini review, Appl. Sci. 9 (2019) 1–17, https://doi.org/10.3390/app9112205.
[2] A.P. Mathew, K. Oksman, M. Sain, Mechanical properties of biodegradable composites from poly lactic acid (PLA) and microcrystalline cellulose (MCC), J. Appl. Polym. Sci. 97 (2005) 2014–2025, https://doi.org/10.1002/app.21779.
[3] A.A.M. Alfayyadh, S. Lotfy, A.A. Basfar, M.I. Khalil, Influences of poly (vinyl alcohol) molecular weight and carbon nanotubes on radiation crosslinking shape memory polymers, Prog. Nat. Sci. Mater. Int. 27 (2017) 316–325, https://doi.org/10.1016/j.pnsc.2017.04.015.
[4] K.J. Narayana, R. Gupta Burela, A review of recent research on multifunctional composite materials and structures with their applications, Mater. Today Proc. 5 (2018) 5580–5590, https://doi.org/10.1016/j.matpr.2017.12.149.
[5] K. Sharma, M.A. Mujawar, A. Kaushik, State-of-art functional biomaterials for tissue engineering, Front. Mater. 6 (2019) 1–10, https://doi.org/10.3389/fmats.2019.00172.
[6] H. Rodríguez-Tobías, G. Morales, D. Grande, Comprehensive review on electrospinning techniques as versatile approaches toward antimicrobial biopolymeric composite fibers, Mater. Sci. Eng. C. 101 (2019) 306–322, https://doi.org/10.1016/j.msec.2019.03.099.
[7] S. Nemati, S. Jeong Kim, Y.M. Shin, H. Shin, Current progress in application of polymeric nanofibers to tissue engineering, Nano Converg. 6 (2019) https://doi.org/10.1186/s40580-019-0209-y.
[8] S.N. Hanumantharao, S. Rao, Multi-functional electrospun nanofibers from, Fibers 7 (2019) 1–35, https://doi.org/10.3390/fib7070066.
[9] Front-matter, in: M. Ramalingam, S. Ramakrishna (Eds.), Nanofiber Compos. Biomed. Appl. Woodhead Publishing 2017, pp. i–iii, https://doi.org/10.1016/b978-0-08-100173-8.00021-1.
[10] J. Yoon, H.S. Yang, B.S. Lee, W.R. Yu, Recent progress in coaxial electrospinning: new parameters, various structures, and wide applications, Adv. Mater. 30 (2018) 1–23, https://doi.org/10.1002/adma.201704765.
[11] H. Qu, S. Wei, Z. Guo, Coaxial electrospun nanostructures and their applications, J. Mater. Chem. A 1 (2013) 11513–11528, https://doi.org/10.1039/c3ta12390a.
[12] H.P. Hinestroza, H. Urena-Saborio, F. Zurita, A.A.G. de León, G. Sundaram, B. Sulbarán-Rangel, Nanocellulose and polycaprolactone nanospun composite membranes and their potential for the removal of pollutants from water, Molecules 25 (2020) https://doi.org/10.3390/molecules25030683.
[13] F. Nejaddehbashi, M. Hashemitabar, V. Bayati, E. Moghimipour, J. Movaffagh, M. Orazizadeh, M. Abbaspour, Incorporation of silver sulfadiazine into an electrospun composite of polycaprolactone as an antibacterial scaffold for wound healing in rats, Cell J. 21 (2020) 379–390, https://doi.org/10.22074/cellj.2020.6341.
[14] R. Dwivedi, S. Kumar, R. Pandey, A. Mahajan, D. Nandana, D.S. Katti, D. Mehrotra, Polycaprolactone as biomaterial for bone scaffolds: review of literature, J. Oral Biol. Craniofacial Res. 10 (2020) 381–388, https://doi.org/10.1016/j.jobcr.2019.10.003.
[15] E. Malikmammadov, T.E. Tanir, A. Kiziltay, V. Hasirci, N. Hasirci, PCL and PCL-Based Materials in Biomedical Applications, Taylor & Francis, 2018 https://doi.org/10.1080/09205063.2017.1394711.
[16] Y. Xu, Y. Xiong, S. Guo, Effect of liquid plasticizers on crystallization of PCL in soft PVC/PCL/plasticizer blends, J. Appl. Polym. Sci. 137 (2020) 34–41, https://doi.org/10.1002/app.48803.
[17] M. Castro, J. Lu, S. Bruzaud, B. Kumar, J.F. Feller, Carbon nanotubes/poly(ε-caprolactone) composite vapour sensors, Carbon N. Y. 47 (2009) 1930–1942, https://doi.org/10.1016/j.carbon.2009.03.037.
[18] Z. Yang, M. Yu, Y. Liu, X. Chen, Y. Zhao, Synthesis and performance of an environmentally friendly polycarboxylate superplasticizer based on modified poly(aspartic acid), Constr. Build. Mater. 202 (2019) 154–161, https://doi.org/10.1016/j.conbuildmat.2018.12.148.
[19] L. Fu, J. Lv, L. Zhou, Z. Li, M. Tang, J. Li, Study on corrosion and scale inhibition mechanism of polyaspartic acid grafted β-cyclodextrin, Mater. Lett. 264 (2020) 127276, https://doi.org/10.1016/j.matlet.2019.127276.
[20] O. Hegedus, D. Juriga, E. Sipos, C. Voniatis, Á. Juhász, A. Idrissi, M. Zrínyi, G. Varga, A. Jedlovszky-Hajdú, K.S. Nagy, Free thiol groups on poly(aspartamide) based hydrogels facilitate tooth-derived progenitor cell proliferation and differentiation, PLoS One 14 (2019) 1–20, https://doi.org/10.1371/journal.pone.0226363.
[21] W. Cho, A New Biocompatible Coating for Bioanalytical Devices Based on PSI (Polysuccinimide), ETD Collect, Purdue Univ, 2020.
[22] K. Molnar, D. Juriga, P.M. Nagy, K. Sinko, A. Jedlovszky-Hajdu, M. Zrinyi, Electrospun poly(aspartic acid) gel scaffolds for artificial extracellular matrix, Polym. Int. 63 (2014) 1608–1615, https://doi.org/10.1002/pi.4720.
[23] K. Molnar, A. Jedlovszky-Hajdu, M. Zrinyi, S. Jiang, S. Agarwal, Poly(amino acid)-based gel fibers with pH responsivity by coaxial reactive electrospinning, Macromol. Rapid Commun. 38 (2017) 1–5, https://doi.org/10.1002/marc.201700147.
[24] C. Voniatis, L. Balsevicius, D. Barczikai, D. Juriga, A. Takács, L. Kőhidai, K. Nagy, A. Jedlovszky-Hajdu, Co-electrospun polysuccinimide/poly(vinyl alcohol) composite meshes for tissue engineering, J. Mol. Liq. 306 (2020)https://doi.org/10.1016/j.molliq.2020.112895.
[25] E. Díaz, I. Sandonis, M.B. Valle, In vitro degradation of poly(caprolactone)/nHA composites, J. Nanomater. 2014 (2014) https://doi.org/10.1155/2014/802435.
[26] A.C. Fonseca, M.H. Gil, P.N. Simões, Biodegradable poly(ester amide)s – a remarkable opportunity for the biomedical area: review on the synthesis, characterization and applications, Prog. Polym. Sci. 39 (2014) 1291–1311, https://doi.org/10.1016/j.progpolymsci.2013.11.007.
[27] D. Juriga, K. Nagy, A. Jedlovszky-Hajdú, K. Perczel-Kovách, Y.M. Chen, G. Varga, M. Zrínyi, Biodegradation and osteosarcoma cell cultivation on poly(aspartic acid) based hydrogels, ACS Appl. Mater. Interfaces 8 (2016) 23463–23476, https://doi.org/10.1021/acsami.6b06489.
[28] T. Elzein, M. Nasser-Eddine, C. Delaite, S. Bistac, P. Dumas, FTIR study of polycaprolactone chain organization at interfaces, J. Colloid Interface Sci. 273 (2004) 381–387, https://doi.org/10.1016/j.jcis.2004.02.001.
[29] A. Benkaddour, K. Jradi, S. Robert, C. Daneault, Grafting of Polycaprolactone on oxidized Nanocelluloses by click chemistry, Nanomaterials. 3 (2013) 141–157, https://doi.org/10.3390/nano3010141.
[30] M. Bagheri, A. Mahmoodzadeh, Polycaprolactone/Graphene Nanocomposites: synthesis, characterization and mechanical properties of electrospun Nanofibers, J. Inorg. Organomet. Polym. Mater. 30 (2020) 1566–1577, https://doi.org/10.1007/s10904-019-01340-8.
[31] S. Il Kim, S.K. Min, J.H. Kim, Synthesis and characterization of novel amino acid-conjugated poly(aspartic acid) derivatives, Bull. Kor. Chem. Soc. 29 (2008) 1887–1892, https://doi.org/10.5012/bkcs.2008.29.10.1887.
[32] N. Tudorachi, A.P. Chiriac, TGA/FTIR/MS study on thermal decomposition of poly (succinimide) and sodium poly(aspartate), Polym. Test. 30 (2011) 397–407, https://doi.org/10.1016/j.polymertesting.2011.02.007.
[33] F. Croisier, A.S. Duwez, C. Jérôme, A.F. Léonard, K.O. Van Der Werf, P.J. Dijkstra, M.L. Bennink, Mechanical testing of electrospun PCL fibers, Acta Biomater. 8 (2012) 218–224, https://doi.org/10.1016/j.actbio.2011.08.015.
[34] A.M. Al-Enizi, M.M. Zagho, A.A. Elzatahry, Polymer-based electrospun nanofibers for biomedical applications, Nanomaterials. 8 (2018) 1–22, https://doi.org/10.3390/nano8040259.
[35] D.P. Bhattarai, L.E. Aguilar, C.H. Park, C.S. Kim, A review on properties of natural and synthetic based electrospun fibrous materials for bone tissue engineering, Membranes (Basel) 8 (2018) https://doi.org/10.3390/membranes8030062.
[36] R. Di Gesù, G. Amato, R. Gottardi, Electrospun scaffolds in tendons regeneration: a review, Muscles Ligam. Tendons J. 9 (2019) 478–493, https://doi.org/10.32098/mltj.04.2019.02.
[37] W. Jiang, J. Shi, W. Li, K. Sun, Morphology, wettability, and mechanical properties of polycaprolactone/hydroxyapatite composite scaffolds with interconnected pore structures fabricated by a mini-deposition system, Polym. Eng. Sci. 52 (2012) 2396–2402, https://doi.org/10.1002/pen.23193.
[38] W. Song, J.F. Mano, Interactions between cells or proteins and surfaces exhibiting extreme wettabilities, Soft Matter 9 (2013) 2985–2999, https://doi.org/10.1039/C3SM27739A.
[39] M. Tallawi, E. Rosellini, N. Barbani, M. Grazia Cascone, R. Rai, G. Saint-Pierre, A.R. Boccaccini, Strategies for the chemical and biological functionalization of scaffolds for cardiac tissue engineering: a review, J. R. Soc. Interface 12 (2015) https://doi.org/10.1098/rsif.2015.0254.
[40] L.A. Bosworth, W. Hu, Y. Shi, S.H. Cartmell, Enhancing biocompatibility without compromising material properties: an optimised NaOH treatment for electrospun Polycaprolactone Fibres, J. Nanomater. 2019 (2019) https://doi.org/10.1155/2019/4605092.
[41] K. Ren, Y. Wang, T. Sun, W. Yue, H. Zhang, Electrospun PCL/gelatin composite nanofiber structures for effective guided bone regeneration membranes, Mater. Sci. Eng. C. 78 (2017) 324–332, https://doi.org/10.1016/j.msec.2017.04.084.
[42] M. Akbarzadeh, M. Pezeshki-Modaress, M. Zandi, Biphasic, tough composite core/shell PCL/PVA-GEL nanofibers for biomedical application, J. Appl. Polym. Sci. 48713 (2019) 1–12, https://doi.org/10.1002/app.48713.
[43] M. Cho, M.A. Karaaslan, S. Renneckar, F. Ko, Enhancement of the mechanical properties of electrospun lignin-based nanofibers by heat treatment, J. Mater. Sci. 52 (2017) 9602–9614, https://doi.org/10.1007/s10853-017-1160-0.